Zirconium and Titanium Complexes Supported by Tridentate LX_2 Ligands Having Two Phenolates Linked to Furan, Thiophene, and Pyridine Donors: Precatalysts for Propylene Polymerization and Oligomerization

Theodor Agapie, Lawrence M. Henling, Antonio G. DiPasquale, Arnold L. Rheingold, and John E. Bercaw*

Arnold and Mabel Beckman Laboratories of Chemical Synthesis, California Institute of Technology, Pasadena, California 91125, and University of California, San Diego, California 92093

Received February 14, 2008

Zirconium and titanium complexes with tridentate bis(phenolate)−donor (donor = pyridine, furan and thiophene) ligands have been prepared and investigated for applications in propylene polymerization. The ligand framework has two "X-type" phenolates connected to the flat heterocyclic "L-type" donor at the 2,6- or 2,5- positions via direct ring−ring (sp^2−sp^2) linkages. The zirconium and titanium dibenzyl complexes have been prepared by treatment of the neutral bis(phenol)−donor ligands with $M(CH_2Ph)_4$ (M = Ti, Zr) with loss of 2 equiv of toluene. Titanium complexes with bis(phenolate)pyridine and -furan ligands and zirconium complexes with bis(phenolate)pyridine and -thiophene ligands have been characterized by single-crystal X-ray diffraction. The solid-state structures of the bis(benzyl)titanium complexes are roughly C_2-symmetric, while the zirconium derivatives display C_s and C_1 symmetry. The bis(phenolate)pyridine titanium complexes are structurally affected by the size of the substituents (CMe_3 or CEt_3) *ortho* to the oxygens, the larger group leading to a larger C_2 distortion. Both titanium and zirconium dibenzyl complexes were found to be catalyst precursors for the polymerization of propylene upon activation with methylaluminoxane (MAO). The activities observed for the zirconium complexes are particularly notable, exceeding 10^6 g polypropylene/mol Zr·h in some cases. The bis(phenolate)pyridine titanium analogues are about 10^3 times less active, but generate polymers of higher molecular weight. When activated with MAO, the titanium bis(phenolate)furan and bis(phenolate)thiophene systems were found to promote propylene oligomerization.

Introduction

Polymers are among the most important commodity chemicals and are produced in quantities of hundreds of billions of pounds per year.[1] The last half-century has seen impressive developments in olefin polymerization catalysis, particularly in the ability to adjust the polymer's architecture, and hence its physical properties, by controlling the structure of the catalyst.[2] It is now possible to rationally design single-site catalysts to control polymer features such as tacticity and level of comonomer incorporation and, to a lesser extent, molecular weight.

Whereas early transition metal metallocene complexes are the most important and best understood structures for single-site catalysts for olefin polymerization,[3,4] nonmetallocene frameworks have recently emerged as versatile alternatives.[5−7] Complexes based on iron, cobalt, nickel, and palladium have been shown to polymerize and oligomerize olefins with good activities, sometimes in a living fashion.[8] In the area of early metal polymerization catalysis, frameworks displaying only one or no cyclopentadienyl ligand have been developed. Various multidentate ligands have been utilized as supporting architectures for olefin polymerization catalysts. In this context, there is increased interest in generating polymers with controlled tacticity through the use of nonmetallocene catalysts.[5,7] Promising advances have been made in both the development of single-site living polymerization catalysts and the design of ancillary ligands that have the appropriate symmetry for polymer tacticity control.[7] While fundamental understanding of the factors responsible for tacticity control generally still lags behind that for metallocene systems, the area of nonmetallocene olefin polymerization catalysis offers the potential for simpler catalyst synthesis and modification, improved activities, and the possibility of producing new polymer architectures.

Anilides and phenolates are common anionic ("X-type") donors in multidentate ligands for polymerization catalysis. Some of the most successful nonmetallocene polymerization catalysts include bi-, tri-, and tetradentate anilide and phenolate ligands. Tridentate bis(anilide) ligands have been reported to support ethylene and α-olefin polymerization; in some cases

* Corresponding author. E-mail: bercaw@caltech.edu.

(1) *Encyclopedia of Polymer Science and Technology*; on-line ed.; Wiley & Sons, Inc.: New York, 2006.

(2) Kissin, Y. V. In *Kirk-Othmer Encyclopedia of Chemical Technology Online*; Wiley & Sons, Inc: New York, 2005.

(3) Coates, G. W. *Chem. Rev.* **2000**, *100*, 1223–1252.

(4) Resconi, L.; Cavallo, L.; Fait, A.; Piemontesi, F. *Chem. Rev.* **2000**, *100*, 1253–1345.

(5) Gibson, V. C.; Spitzmesser, S. K. *Chem. Rev.* **2003**, *103*, 283–315.

(6) Britovsek, G. J. P.; Gibson, V. C.; Wass, D. F. *Angew. Chem., Int. Ed.* **1999**, *38*, 428–447.

(7) Coates, G. W.; Hustad, P. D.; Reinartz, S. *Angew. Chem., Int. Ed.* **2002**, *41*, 2236–2257.

(8) Ittel, S. D.; Johnson, L. K.; Brookhart, M. *Chem. Rev.* **2000**, *100*, 1169–1203.

10.1021/om800136y CCC: $40.75
Publication on Web 11/06/2008

Scheme 1

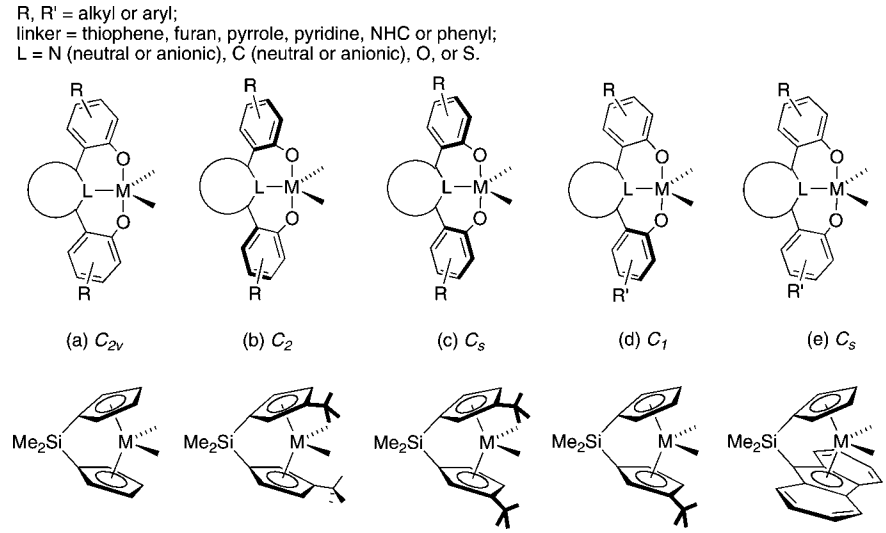

living polymerization of 1-hexene was possible.[9−15] Bidentate imino-phenolate ligands have been shown to support C_2-symmetric architectures; these catalysts are able to generate syndiotactic or isotactic polypropylene depending on the nature of the substituents on the phenolate rings.[16−21] Tetradentate bis(phenolate) frameworks have been reported to support very active catalysts for the polymerization of 1-hexene; again, tacticity control was possible by use of C_2-symmetric architectures.[22−31] Tridentate bis(phenolate) frameworks have been successful as well in supporting olefin polymerization.[32−35]

Zirconium bis(phenoxy)pyridine precatalysts were shown to polymerize ethylene with high activities and also incorporate propylene.[34,35] A chiral cationic zirconium bis(alkoxy)pyridine complex was found to insert only one ethylene molecule,[36] while a related titanium bis(alkoxy)pyridine was reported to polymerize ethylene with good activity.[37] A zirconium bis(anilidyl)pyridine system was shown to polymerize ethylene upon activation with MAO.[38] Notably, computational studies on multidentate bis(phenoxide) ligand systems indicated that a strong interaction with the additional donor lowers the transition state for olefin insertion.[39] Thus, whereas chelating ligands having phenolate or anilide substituents are often suitable for early transition metal catalysts for olefin polymerizations, the factors governing activity and tacticity are, for the most part, unpredictable. A more systematic approach to ligand design could well provide the basis for predicting these catalyst characteristics.

Herein we report the development of versatile tridentate bis(phenolate)−donor ligand architectures that afford active catalysts for the polymerization of propylene when metalated with titanium or zirconium. The ligand framework has two phenolates connected to a flat heterocyclic ("L-type") donor (pyridine, furan, or thiophene) at the 2,6- or 2,5-positions via direct ring−ring (sp^2−sp^2) linkages. Variants of this LX_2 ligand utilizing a pyridine linker and two phenoxides were reported by other groups to bind to iron(III), copper(II), and aluminum(III) in a C_2 fashion,[40] whereas when bound to boron or

(9) Baumann, R.; Stumpf, R.; Davis, W. M.; Liang, L. C.; Schrock, R. R. *J. Am. Chem. Soc.* **1999**, *121*, 7822–7836.
(10) Liang, L. C.; Schrock, R. R.; Davis, W. M.; McConville, D. H. *J. Am. Chem. Soc.* **1999**, *121*, 5797–5798.
(11) Aizenberg, M.; Turculet, L.; Davis, W. M.; Schattenmann, F.; Schrock, R. R. *Organometallics* **1998**, *17*, 4795–4812.
(12) Baumann, R.; Davis, W. M.; Schrock, R. R. *J. Am. Chem. Soc.* **1997**, *119*, 3830–3831.
(13) Mehrkhodavandi, P.; Schrock, R. R.; Pryor, L. L. *Organometallics* **2003**, *22*, 4569–4583.
(14) Mehrkhodavandi, P.; Schrock, R. R. *J. Am. Chem. Soc.* **2001**, *123*, 10746–10747.
(15) Mehrkhodavandi, P.; Bonitatebus, P. J.; Schrock, R. R. *J. Am. Chem. Soc.* **2000**, *122*, 7841–7842.
(16) Mason, A. F.; Coates, G. W. *J. Am. Chem. Soc.* **2004**, *126*, 16326–16327.
(17) Mason, A. F.; Coates, G. W. *J. Am. Chem. Soc.* **2004**, *126*, 10798–10799.
(18) Reinartz, S.; Mason, A. F.; Lobkovsky, E. B.; Coates, G. W. *Organometallics* **2003**, *22*, 2542–2544.
(19) Mitani, M.; Furuyama, R.; Mohri, J.; Saito, J.; Ishii, S.; Terao, H.; Nakano, T.; Tanaka, H.; Fujita, T. *J. Am. Chem. Soc.* **2003**, *125*, 4293–4305.
(20) Tian, J.; Hustad, P. D.; Coates, G. W. *J. Am. Chem. Soc.* **2001**, *123*, 5134–5135.
(21) Tian, J.; Coates, G. W. *Angew. Chem., Int. Ed.* **2000**, *39*, 3626–3629.
(22) Segal, S.; Goldberg, I.; Kol, M. *Organometallics* **2005**, *24*, 200–202.
(23) Groysman, S.; Tshuva, E. Y.; Goldberg, I.; Kol, M.; Goldschmidt, Z.; Shuster, M. *Organometallics* **2004**, *23*, 5291–5299.
(24) Tshuva, E. Y.; Groysman, S.; Goldberg, I.; Kol, M.; Goldschmidt, Z. *Organometallics* **2002**, *21*, 662–670.
(25) Tshuva, E. Y.; Goldberg, I.; Kol, M.; Goldschmidt, Z. *Chem. Commun.* **2001**, 2120–2121.
(26) Tshuva, E. Y.; Goldberg, I.; Kol, M.; Goldschmidt, Z. *Organometallics* **2001**, *20*, 3017–3028.
(27) Tshuva, E. Y.; Goldberg, I.; Kol, M. *J. Am. Chem. Soc.* **2001**, *123*, 3621–3621.
(28) Tshuva, E. Y.; Goldberg, I.; Kol, M.; Goldschmidt, Z. *Inorg. Chem. Commun.* **2000**, *3*, 611–614.
(29) Tshuva, E. Y.; Goldberg, I.; Kol, M. *J. Am. Chem. Soc.* **2000**, *122*, 10706–10707.
(30) Tshuva, E. Y.; Goldberg, I.; Kol, M.; Weitman, H.; Goldschmidt, Z. *Chem. Commun.* **2000**, 379–380.
(31) Tshuva, E. Y.; Versano, M.; Goldberg, I.; Kol, M.; Weitman, H.; Goldschmidt, Z. *Inorg. Chem. Commun.* **1999**, *2*, 371–373.
(32) Takaoki, K.; Miyatake, T. *Macromol. Symp.* **2000**, *157*, 251–257.
(33) Nakayama, Y.; Watanabe, K.; Ueyama, N.; Nakamura, A.; Harada, A.; Okuda, J. *Organometallics* **2000**, *19*, 2498–2503.
(34) Chan, M. C. W.; Tam, K. H.; Pui, Y. L.; Zhu, N. Y. *J. Chem. Soc., Dalton Trans.* **2002**, 3085–3087.
(35) Chan, M. C. W.; Tam, K. H.; Zhu, N. Y.; Chiu, P.; Matsui, S. *Organometallics* **2006**, *25*, 785–792.
(36) Gauvin, R. M.; Osborn, J. A.; Kress, J. *Organometallics* **2000**, *19*, 2944–2946.
(37) Mack, H.; Eisen, M. S. *J. Chem. Soc., Dalton Trans.* **1998**, 917–921.
(38) Guerin, F.; McConville, D. H.; Vittal, J. J. *Organometallics* **1996**, *15*, 5586–5590.
(39) Froese, R. D. J.; Musaev, D. G.; Morokuma, K. *Organometallics* **1999**, *18*, 373–379.
(40) Steinhauser, S.; Heinz, U.; Sander, J.; Hegetschweiler, K. *Z. Anorg. Allg. Chem.* **2004**, *630*, 1829–1838.

Scheme 2

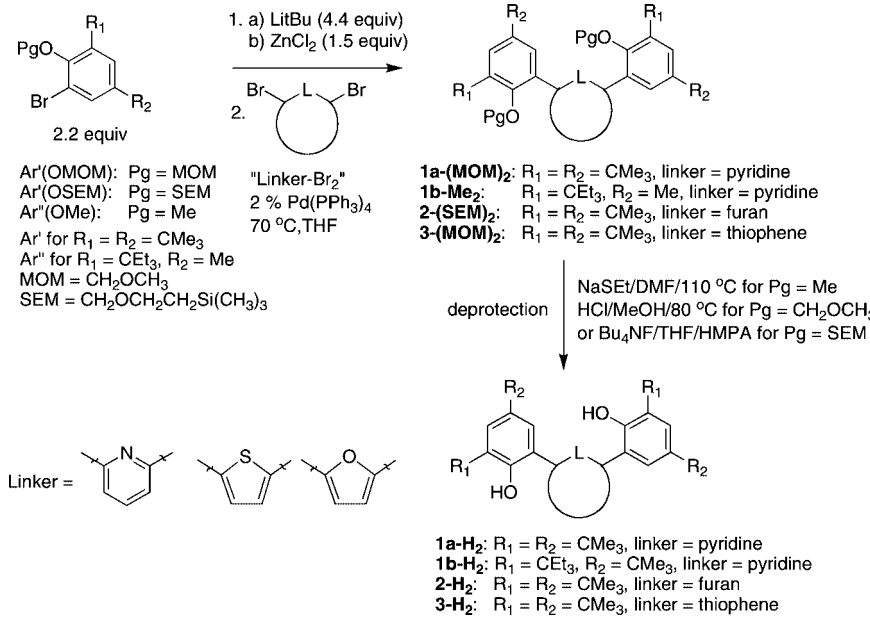

zirconium(IV), this ligand binds in a C_s fashion.[34,35,41] We have found in a related study that these LX_2 type (or X_3 type, when the linking ligand is a 2,6-disubstituted phenyl) ligands bind to tantalum meridionally, giving rise to diverse symmetries at the metal center,[42] that relate them structurally to appropriately substituted *ansa*-metallocene systems (Scheme 1). Preliminary studies reveal that the propylene polymerization activities for the zirconium complexes are particularly high, exceeding 10^6 g polypropylene/mol Zr·h in some cases. On the other hand, the resulting polypropylenes are essentially stereoirregular for polymers produced with catalysts having these ligand architectures.

Results and Discussion

Preparation of Diphenols. The bis(phenol)pyridines, -furans, and -thiophenes were prepared using well-established procedures. Starting from commercially available and inexpensive 2,4-di-*tert*-butylphenol, the desired linked diphenols can be accessed in only four steps. Bromination and suitable protection of the phenol functionality generates precursors for palladium coupling chemistry (Scheme 2). Lithium−halogen exchange, followed by salt metathesis with $ZnCl_2$, provides, *in situ*, aryl zinc reagents suitable for the Negishi cross-coupling. 2,6-Dibromopyridine, 2,5-dibromothiophene, and 2,5-dibromofuran have been used as coupling partners with $Pd(PPh_3)_4$ as catalyst. Aqueous workup provides protected diphenols as white powders. Methyl and methoxymethyl (MOM) protecting groups have been used for making the pyridine and thiophene linked systems. Standard deprotecting procedures—acidic methanol at 80 °C; NaSEt in DMF at 110 °C—have been employed for removing MOM and Me groups, respectively. For the furan-linked system, acid-catalyzed removal of MOM groups proved difficult, leading to multiple products. Utilization of SEM protecting groups allowed both the palladium-catalyzed coupling reaction and clean deprotection using Bu_4NF in hexamethylphosphoramide (HMPA). Analytically pure linked diphenols are obtained as white solids by precipitation from methanol and collection by filtration.

Preparation of Zirconium and Titanium Complexes Supported by Tridentate Bis(phenolate)−Donor Ligands. Titanium and zirconium dibenzyl complexes have been prepared by toluene elimination in reaction of the tetrabenzyl precursors and bis(phenol)−donor ligands in diethyl ether solution (eq 1). The titanium complexes are obtained as orange (**1a-TiBn$_2$** and **1b-TiBn$_2$**, Bn = benzyl) or red (**2-TiBn$_2$** and **3-TiBn$_2$**) solids, while the zirconium complexes are pale yellow (**1a-ZrBn$_2$**, **1b-ZrBn$_2$**, and **3-ZrBn$_2$**) or colorless (**2-ZrBn$_2$**). Coordinated ether was not observed by NMR spectroscopy, indicating that the products are likely five-coordinate. ^{1}H NMR spectra of the titanium and zirconium dibenzyl complexes show a singlet for the benzyl CH_2 protons. A variable-temperature ^{1}H NMR study was performed for **1a-TiBn$_2$**. The benzyl peak was found to remain a sharp singlet at temperatures as low as −80 °C.

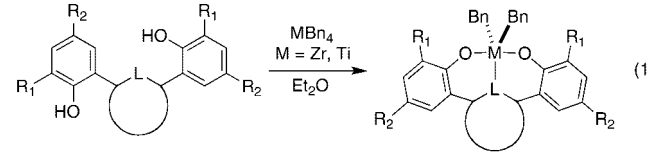

1a-H$_2$: R$_1$ = R$_2$ = CMe$_3$, linker = pyridine
1b-H$_2$: R$_1$ = CEt$_3$, R$_2$ = Me, linker = pyridine
2-H$_2$: R$_1$ = R$_2$ = CMe$_3$, linker = furan
3-H$_2$: R$_1$ = R$_2$ = CMe$_3$, linker = thiophene

1a-TiBn$_2$ **1a-ZrBn$_2$**
1b-TiBn$_2$ **1b-ZrBn$_2$**
2-TiBn$_2$ **2-ZrBn$_2$**
3-TiBn$_2$ **3-ZrBn$_2$**

As has been shown for tantalum,[42] these ligands can achieve a number of binding geometries (C_{2v}, C_s, C_2, C_1) that may, in principle, be distinguishable by ^{1}H NMR spectroscopy through analysis of the benzyl [CH_2] protons: (1) a C_{2v} geometry is expected to lead to a singlet for these protons, (2) a C_s geometry should display two singlets, (3) a C_2 symmetry makes the [CH_2] protons diastereotopic, which should lead to two doublets, and (4) a C_1 geometry would make all four benzylic protons different, leading to four doublets. The observed ^{1}H NMR spectra of the titanium and zirconium dibenzyl complexes showing only a singlet for the benzyl [CH_2] protons suggest that the solution structures are either C_{2v}-symmetric or in fast exchange between different possible geometries (Scheme 3). The ^{1}H NMR spectrum for **1a-TiBn$_2$** at −80 °C shows a sharp singlet for the [CH_2] protons, indicating that if an exchange occurs, its barrier is rather small (less than ∼8 kcal·mol^{-1}). Scheme 3 shows the interconversion between the C_{2v}, C_s, and

(41) Li, Y. Q.; Liu, Y.; Bu, W. M.; Guo, J. H.; Wang, Y. *Chem. Commun.* **2000**, 1551–1552.
(42) Agapie, T.; Day, M. W.; Bercaw, J. E. *Organometallics* **2008**, accepted.

Scheme 3

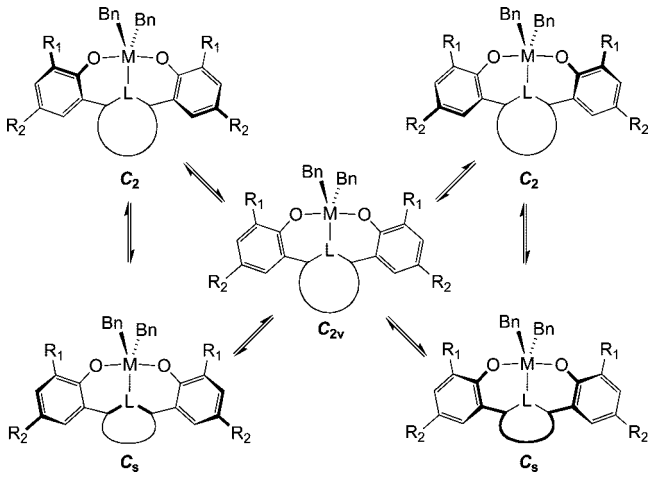

C_2 geometries; the C_1 geometry is not shown, being intermediate between the other three. While it is not clear which geometry should be preferred, the structures of the tantalum complexes suggest that this will be dependent on the type of linker involved.[42] Exchange between C_2 enantiomers could occur via a C_{2v} structure, if both phenolate rings twist simultaneously, or via C_1 structures, if the rings twist separately. Similarly, exchange between the two C_s structures can occur via C_{2v} or C_1 intermediates.

The solution symmetry of these complexes and their ability to exchange between different geometries may be important with regard to controlling polymer microstructure. For example, a C_2 structure may enforce isotactic polymerization, if the transfer of ligand steric interactions to the metal site is efficient enough, while the C_s and C_{2v} structures shown above should give atactic polymers. If $C_2 \leftrightarrow C_s$ interconversion occurs at a rate slower than the insertion rates, stereoblock polymers could be obtained, if enantiomorphic site control is operative. A similar type of oscillation of the catalyst has been proposed to lead to isotactic−atactic stereoblock polypropylene.[43−45] In a related process, inversion between the two C_2 structures could be controlled by the polymer chain end. In this case, syndiotactic polymer could be generated, if the inversion occurs after each enchainment of α-olefin.[46,47]

As a measure of ligand steric demands, the ability to coordinate two bis(phenolate)pyridine ligands per metal was investigated. Reaction of tetrabenzyl precursors was performed with 2 equiv of **1a-H$_2$**. For zirconium, a mixture of species is generated within a few hours (^{1}H NMR spectroscopy), displaying the free phenol, **1a-ZrBn$_2$**, as well as another species assigned as **(1a)$_2$-Zr**. Upon heating to 60 °C for 10.5 h, this mixture funnels to one species displaying no benzyl peaks, but only signals attributable to coordinated **1a**, consistent with the clean formation of **(1a)$_2$-Zr**. An analogous experiment was performed with titanium. At room temperature reaction with $TiBn_4$ generates only the titanium dibenzyl species (**1a-Ti**) and leaves an equivalent of bis(phenol)pyridine unreacted. Heating at 60 °C for 10.5 h leads to a new species with no benzyl peaks, but **1a-Ti** remains. Extending the reaction time by 24 h leads to complete conversion to the tetraphenolate complex **(1a)$_2$-Ti**. The fact that titanium(IV) and zirconium(IV) can coordinate two bis(phenolate)pyridine ligands indicates that while the 2,6-substituents impart some steric bulk to the ligand, the metal center still remains quite open out of the plane of the [**M−1a**] plane. That the reaction for titanium is slower than for zirconium may indicate that its rate is controlled largely by sterics.

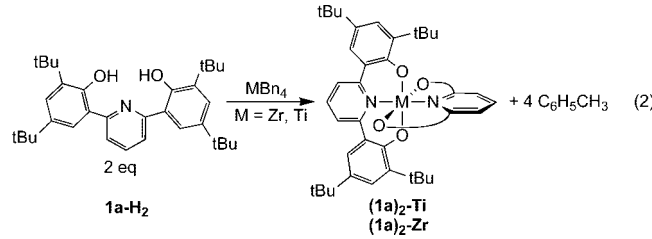

(2)

Structural Characterization of Group 4 Dibenzyl Complexes with Tridentate Diphenolate Ligands. Single-crystal X-ray diffraction studies have been instrumental in determining the binding modes of these bis(phenolate)−donor ligands, although, of course, these structures are for the solid state, and thus may not necessarily reflect the preferred geometries in solution. Attempts to grow crystals adequate for these studies were successful for compounds **1a-TiBn$_2$**, **1b-TiBn$_2$**, **2-TiBn$_2$**, **1b-ZrBn$_2$**, and **3-ZrBn$_2$**. All three titanium complexes were found to be five-coordinate in the solid state, with an approximate trigonal-bipyramidal geometry. The two phenolate rings twist away from each other to give rise to C_2-symmetric structures. The dihedral angles between the Ti−O bonds and the plane of the linker may be used as a measure of the twisting (the twist angles in Table 1) for the C_2 structure. Keeping the linker the same (pyridine, for **1a-TiBn$_2$**, Figure 1, and for **1b-TiBn$_2$**, Figure 2) allows for a comparison of the effect of substituents *ortho* to the phenolate oxygen. Switching from [CMe_3] to [CEt_3] leads to an increase in the twist angle by about 8°, from about 28° to 36°. The distance between the quaternary carbons of the *ortho* CMe_3 or CEt_3 substituents (d_{C-C}) changes by less than 0.1 Å. Not surprisingly, the distance between the phenolate oxygens (d_{O-O}) does not change significantly. The interaction of the metal with the benzyl groups is notable: for **1a-TiBn$_2$** the Ti−C−C_{ipso} angles of the [$TiCH_2C_6H_5$] moieties are around 97°, while for **1b-TiBn$_2$** they are 108° and 114°; the Ti−C_{ipso} distance varies accordingly (Table 1). These structural features indicate that the steric bulk of the substituent in the *ortho* position affects both the orientation of the biphenolate framework and the binding of the other ligands. Increasing the steric bulk forces the phenolate rings to twist further away from each other, but the distance between the phenolate *ortho* substituents is not affected significantly. The bulkier CEt_3 group also has the effect of pushing the phenyl of the benzyl ligands away from the metal center and away from an η^2-benzyl coordination. Interestingly, the orientation of the two benzyl groups is more propeller-like in the less bulky system, **1a-TiBn$_2$**, possibly indicating that the large CEt_3 groups in **1b-TiBn$_2$** reach to the benzyl phenyl ring on both sides of the bis(phenolate)pyridine ligand, pushing it away from the preferred propeller orientation. It is noteworthy that the C_2 binding mode of the ligand is in contrast to its C_s binding mode in all tantalum complexes,[42] indicating that the symmetry of the metal complex can be tuned, possibly by changing the size of the central atom via using different metals and/or different oxidation states.

(43) Coates, G. W.; Waymouth, R. M. *Science* **1995**, *267*, 217–219.
(44) Busico, V.; Castelli, V. V. A.; Aprea, P.; Cipullo, R.; Segre, A.; Talarico, G.; Vacatello, M. *J. Am. Chem. Soc.* **2003**, *125*, 5451–5460.
(45) Busico, V.; Cipullo, R.; Kretschmer, W. P.; Talarico, G.; Vacatello, M.; Castelli, V. V. *Angew. Chem., Int. Ed.* **2002**, *41*, 505–508.
(46) Tian, J.; Hustad, P. D.; Coates, G. W. *J. Am. Chem. Soc.* **2001**, *123*, 5134–5135.
(47) Milano, G.; Cavallo, L.; Guerra, G. *J. Am. Chem. Soc.* **2002**, *124*, 13368–13369.

Table 1. Selected Structural Parameters for the Crystallographically Characterized Group 4 Compounds Supported by Tridentate Bis(phenolate) Frameworks[a]

compound	twist angles (deg)	d_{OO} (Å)	d_{CC} (Å)	M−C (Å)	M−C_{ipso} (Å)	M−C−C_{ipso} (deg)
1a-TiBn$_2$	27.6	3.70	9.11	2.12	2.74	96.9
	28.2			2.12	2.73	97.4
1b-TiBn$_2$	35.3	3.74	9.15	2.10	3.03	114.0
	36.1			2.12	2.93	107.6
2-TiBn$_2$	21.6	3.64	11.29	2.09	2.61	91.8
	25.4			2.11	2.64	93.4
1b-ZrBn$_2$(OEt$_2$)		3.9	9.44	2.29	2.676	103.9
				2.33	3.41	125.8
3-ZrBn$_2$		3.86	9.38	2.26	2.60	85.3
				2.27	2.95	102.4

[a] The twist angle is the dihedral angle between a M−O bond and the plane of the heterocyclic donor ring; d_{O-O} is the distance between the phenolate oxygens; d_{C-C} is the distance between the quaternary carbons of the *ortho* CMe_3 or CEt_3 substituents.

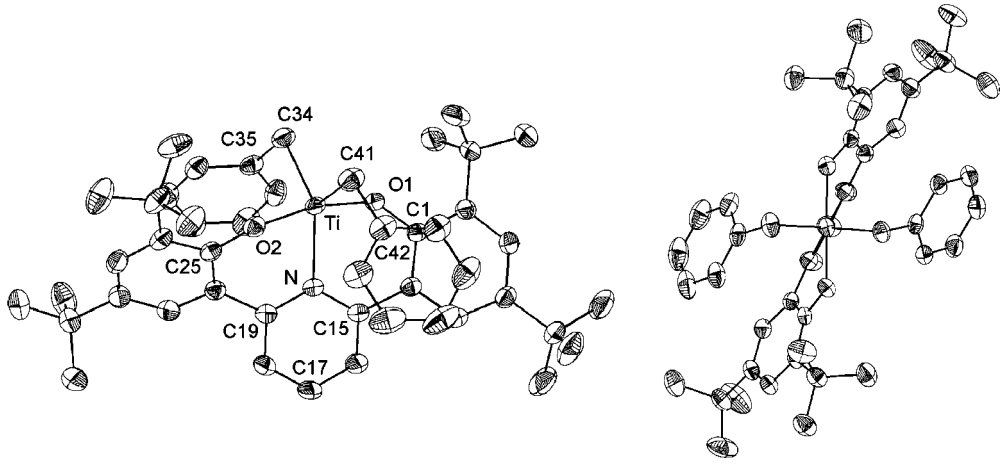

Figure 1. Drawings of the structure of **1a-TiBn$_2$**. Selected bond lengths (Å) and angles (deg): N(1)−Ti(1) 2.2181(12); O(1)−Ti(1) 1.8688(11); O(2)−Ti(1) 1.8578(11); C(34)−Ti(1) 2.1222(17); C(41)−Ti(1) 2.1207(16); C(35)−C(34)−Ti(1) 96.92(10); C(42)−C(41)−Ti(1) 97.43(10); C(1)−O(1)−Ti(1) 132.47(10); C(25)−O(2)−Ti(1) 134.96(10).

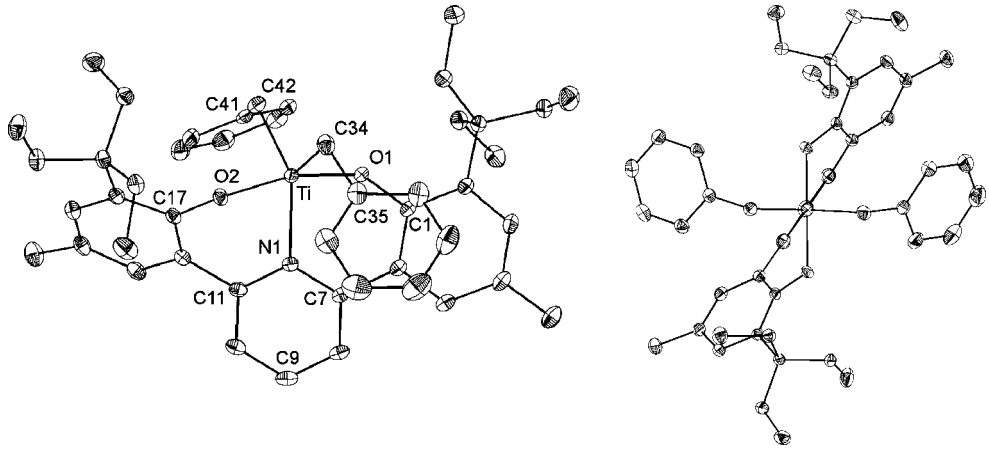

Figure 2. Drawings of the structure of **1b-TiBn$_2$**. Selected bond lengths (Å) and angles (deg): Ti(1)−O(1) 1.8873(7); Ti(1)−O(2) 1.8935(8); Ti(1)−C(41) 2.1022(10); Ti(1)−C(34) 2.1167(10); Ti(1)−N(1) 2.1587(8); O(1)−Ti(1)−O(2) 164.93(3); C(35)−C(34)−Ti(1) 107.67(7); C(42)−C(41)−Ti(1) 114.04(7); C(1)−O(1)−Ti(1) 126.24(6); C(17)−O(2)−Ti(1) 123.38(6).

Comparison between **1a-TiBn$_2$** and **2-TiBn$_2$** (Figure 3) allows for the study of the effect of changing the linker while keeping the phenolate *ortho* substituents the same (CMe_3). Moving from pyridine to furan causes a small decrease in the twist angle (from 28° to about 24°, Table 1). However, the distance between the *ortho* stubstituents (d_{C-C}) increases substantially, by more than 2 Å from 9.11 Å to 11.29 Å; this is probably a consequence of the five-membered ring furan linker, which pushes the phenolate rings out, making the metal center more open. The Ti−C−C_{ipso} angles for the [Ti$CH_2C_6H_5$] moieties are slightly smaller in the furan-based system, likely a consequence of the less sterically hindered environment around the metal or a result of a more electrophilic metal center with a furan donor versus the pyridine donor.

The X-ray structures show that the zirconium complexes have C_s- (**1b-ZrBn$_2$·OEt$_2$**, Figure 4) and C_1-symmetric (**3-ZrBn$_2$**, Figure 5) binding modes of the LX_2 ligand. Crystals of the bis(phenolate)pyridine-ligated complex (**1b-ZrBn$_2$**) were obtained from a saturated diethyl ether solution, and a molecule of ether was found coordinated to zirconium, leading to a distorted octahedral geometry. One of the Zr−C_{ipso} distances of the [Zr$CH_2C_6H_5$] moieties is longer than the other by over

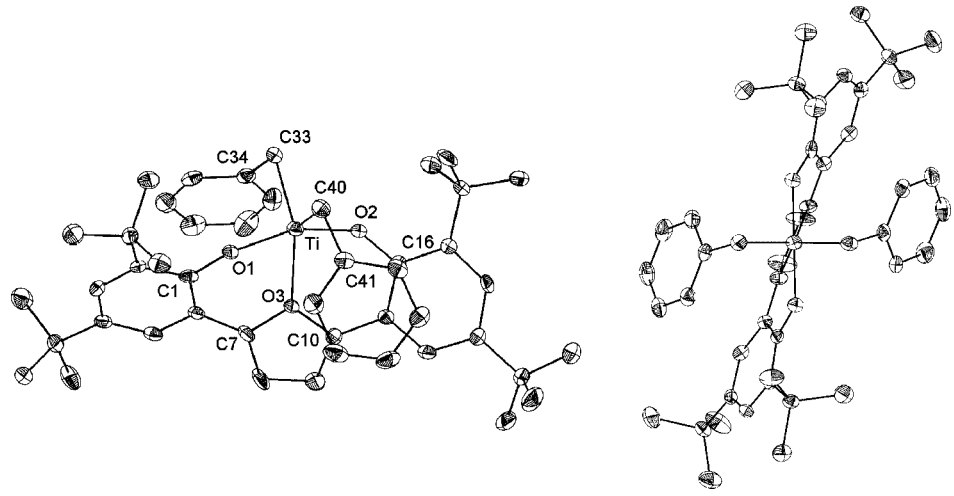

Figure 3. Drawings of the structure of **2-TiBn$_2$**. Selected bond lengths (Å) and angles (deg): Ti(1)−O(2) 1.8605(16); Ti(1)−O(1) 1.8576(16); Ti(1)−C(33) 2.094(2); Ti(1)−C(40) 2.105(2); Ti(1)−O(3) 2.2510(15); Ti(1)−C(34) 2.605(3); Ti(1)−C(41) 2.641(2); O(2)−Ti(1)−O(1) 157.26(7); C(1)−O(1)−Ti(1) 140.67(15); C(16)−O(2)−Ti(1) 140.08(15); C(34)−C(33)−Ti(1) 91.80(14); C(41)−C(40)−Ti(1) 93.37(15).

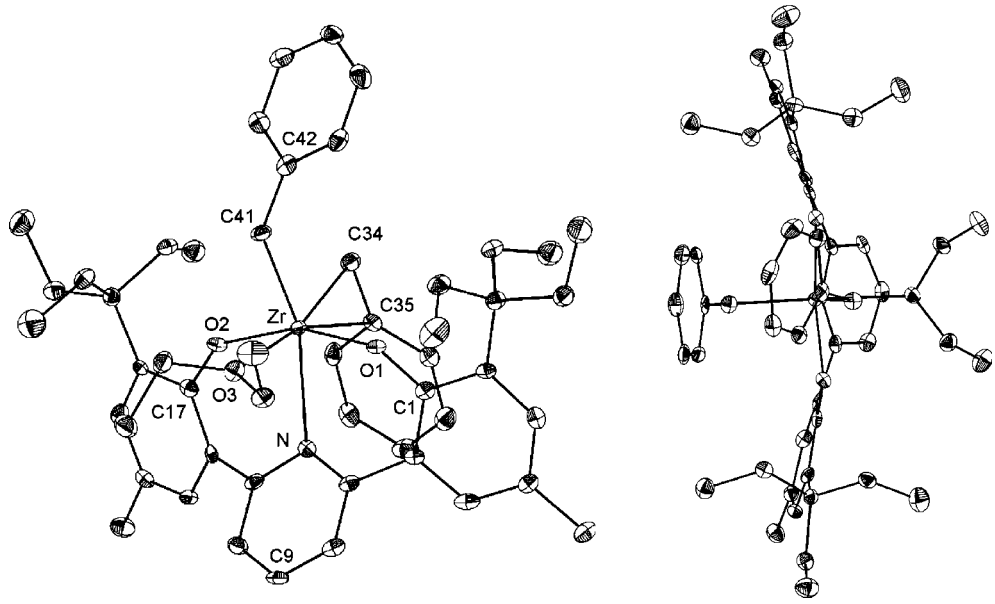

Figure 4. Drawings of the structure of **1b-ZrBn$_2$(OEt$_2$)**. Selected bond lengths (Å) and angles (deg): Zr(1)−O(2) 1.9797(16); Zr(1)−O(1) 1.9897(15); Zr(1)−C(34) 2.289(3); Zr(1)−C(41) 2.334(3); Zr(1)−O(3) 2.3907(16); Zr(1)−N(1) 2.471(2); Zr(1)−C(35) 2.676(2); O(2)−Zr(1)−O(1) 158.67(7); C(1)−O(1)−Zr(1) 142.84(14); C(17)-O()-Zr(1) 143.80(16); C(36)−C(35)−Zr(1) 103.86(16); C(42)−C(41)−Zr(1) 125.62(18).

0.7 Å. The pyridine plane is tilted away from the Zr−N vector, and the Zr−N bond length is long. As in the case of tantalum complexes supported by the same ligand, bending of the pyridine ring away from the M−N vector relieves some of the strain of the unnaturally short metal−nitrogen interaction and results in C_s-symmetric structures.[42] The long zirconium−O_{ether} bond length is indicative of a weak interaction, consistent with the fact that the ether can be removed under vacuum. The metal center's electrophilicity is indicated by the one relatively short Zr−C_{ipso} distance.

The thiophene-bridged bis(phenolate)zirconium dibenzyl complex **3-ZrBn$_2$** was crystallized from toluene. Its structure is a distorted trigonal bipyramid with the bis(phenolate)thiophene ligand binding in a C_1-fashion. The structural features of the two phenolate ligands are similar to the ones observed for the tantalum complex supported by the same ligand.[42] The thiophene ring is almost perpendicular to the Zr−S vector. One of the benzyl groups significantly bends toward the metal center to give a Zr−C−C_{ipso} angle of 85.3° and a short Zr−C_{ipso} distance of 2.60 Å. The zirconium center supported by the bis(phenolate)thiophene ligand appears to be more electrophilic than in corresponding bis(phenolate)pyridine system, as indicated by the stronger interaction with benzyl *ipso*-carbon. This higher electrophilicity is almost certainly due to the fact that the thiophene system is five-coordinate (lacking the coordinated ether of **1b-ZrBn$_2$·OEt$_2$**), but also possibly to a weaker interaction of the metal center with the sulfur compared to the nitrogen donor.

Overall, bis(phenolate)−donor ligand binding modes for the zirconium complexes were found to be more similar to the tantalum complexes than the titanium complexes, suggesting that the ligand binding mode may be more dependent on the size of the metal center than on coordination number. Importantly, both titanium and zirconium complexes show meridional

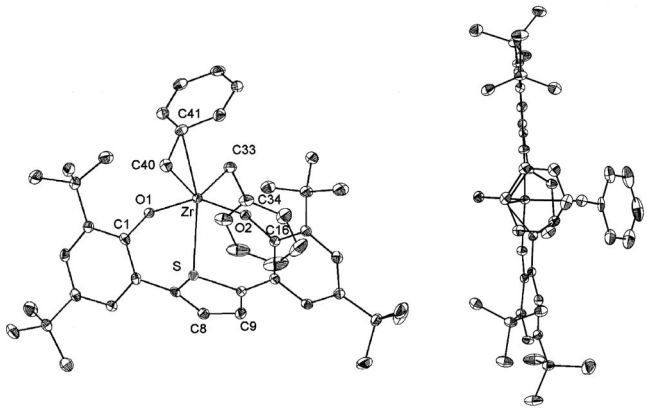

Figure 5. Drawings of the structures of **3-ZrBn$_2$**. Selected bond lengths (Å) and angles (deg): Zr(1)−O(2) 1.9999(11); Zr(1)−O(1) 2.0052(11); Zr(1)−C(33) 2.259(2); Zr(1)−C(40) 2.273(2); Zr(1)−C(41) 2.5973(17); Zr(1)−S(1) 2.6411(5); O(2)−Zr(1)−O(1) 149.24(5); C(1)−O(1)−Zr(1) 153.07(11); C(16)−O(2)−Zr(1) 152.35(10); C(41)−C(40)−Zr(1) 85.25(11); C(34)−C(33)−Zr(1) 102.41(12).

binding of the multidentate ligands, which, if general, should limit the number of possible accessible geometries during catalysis. Related, more flexible bis(anilide) tridentate ligands, investigated by Schrock et al., were shown to bind in both *fac* and *mer* fashion (with some exceptions), which could diminish polymer tacticity control.[9,12] It is noteworthy that in solution these complexes are fluxional, based on the NMR features, *vis-à-vis* solid-state structures. Thus, various symmetries may be accessed in the solution state (*vide supra*).

Propylene Polymerization and Oligomerization with Zirconium Complexes. Propylene polymerization trials have been performed at 0 °C, upon activation of these bis(phenolate)−donor ligated dibenzyl complexes with excess methylaluminumoxane (MAO) in toluene solution (Table 2). The zirconium species generate waxy polymers, which may be separated from the quenched methanol/hydrochloric acid mixture by decantation. The purified polymers have been analyzed by ^{1}H and ^{13}C NMR spectroscopy (see Supporting Information for representative examples), GPC, and GC-MS. These polymerization systems proved to be very active, in some cases exceeding 10^6 g polypropylene/(mol Zr·h), comparable to some of the most active propylene polymerization catalysts known (for example a double *ansa* zirconocene catalyst has an activity of 10^6 g/mol h at 0 °C with 2000 equiv of MAO).[48]

Interestingly, the polymer molecular weight distributions for the polypropylenes obtained from the zirconium pyridine−bisphenolate systems (**1a-ZrBn$_2$** and **1b-ZrBn$_2$**) are bimodal (GPC), with both fractions displaying low PDIs (Figure 6). For polymers obtained from **1a-ZrBn$_2$**, the high molecular weight fractions (MW = (1.6−1.9) × 10^5) were found to have PDIs between 1.9 and 2.5, while the low molecular weight ones are around 1.5 (MW ≈ 1.3 × 10^5). On varying the MAO excess from 2000 to 4000 equiv, the molecular weight distribution shifts toward lower molecular weight (Figure 6). ^{13}C NMR analysis of the resulting polymers shows significant peaks corresponding to isobutyl terminal groups, peaks that increased in propensity with increasing MAO excess (Figure 7).[49,50] The polymerization activity was found to be dependent on MAO excess, with maximum activities at intermediate MAO excess. Polymers generated from **1b-ZrBn$_2$** or from **1a-ZrBn$_2$** with 500 equiv of MAO have few isobutyl end groups (^{13}C NMR spectroscopy), but display terminal and internal olefin peaks as well as *n*-propyl end groups. Based on ^{13}C NMR spectroscopic analysis, the obtained polymers are stereoirregular. GC-MS analysis revealed that polymers from **1b-ZrBn$_2$** display some low molecular weight oligomers of propylene ($C_{<30}$).

The small PDIs observed for each polymer fraction are indicative of single-site catalysts. The observed bimodal distribution is probably due to the presence of two types of catalysts, the relative distribution of which is dependent on the amount of MAO utilized. An alternative explanation involves rapid chain transfer to MAO Al-Me groups; once these groups are converted to Al-polymeryl, chain shuttling is slower, leading to higher molecular weight polymers. The presence of isobutyl terminal groups is indicative of chain transfer to aluminum. If 1,2-insertion is the propagation regiochemistry, then isobutyl terminal groups could form at both ends of the polymer, by insertion into the initial [Zr−Me], bond as well as by chain transfer of a [CH_2CH(Me)(polymeryl)] group from zirconium to aluminum followed by quenching by acid (Scheme 4). The increase in the isobutyl end groups with increasing the excess MAO is consistent with an increased amount of chain transfer to aluminum. The diverse set of olefin resonances observed in some of the samples may be indicative of metal chain-walking or possibly of acid-catalyzed isomerization upon workup. Samples that show signals attributable to olefinic carbons (^{13}C NMR spectroscopy) were also found to show a similar amount of *n*-propyl end groups, consistent with termination events based on β-H elimination and with 1,2-insertion of propylene into the generated metal hydride. The observed predominant end groups are consistent with a preference for 1,2-insertion of propylene into both [Zr−H] and [Zr−C] bonds.

The differences in behavior between **1a-ZrBn$_2$** and **1b-ZrBn$_2$**, with regard to the presence of oligomers, isobutyl end groups, effect of excess MAO, and propensity for β-H elimination, could rise from a variety of reasons. For example the bulkier system **1b-ZrBn$_2$** may hinder chain transfer to aluminum, and hence decrease the number of isobutyl end groups. However, this does not account for the formation of low MW oligomers of propylene and increase in β-H elimination events. A broader pool of ligand frameworks needs to be explored before conclusions can be drawn.

To investigate the ability of the zirconium bis(phenolate)pyridine systems to support polymerization catalysis upon stoichiometric activation, the reaction of **1b-ZrBn$_2$** with [Ph_3C][$B(C_6F_5)_4$] was performed in C_6D_5Cl, in a J-Young tube. This reaction is not clean, but formation of one major species was observed by ^{1}H NMR spectroscopy. Excess 1-hexene was added to the mixture and allowed to react for 3 h. ^{1}H NMR spectroscopy shows almost complete disappearance of the 1-hexene peaks and appearance of new signals in the olefin region. On the basis of the integrals of the vinyl region versus the aliphatic region, the oligomers formed contain on average 15 1-hexene monomers. After allowing to stand at room temperature for a day, another portion of 1-hexene was added and consumption of the monomer was observed again (the second time to a lower extent). These observations indicate that the cationic zirconium species resulting from stoichiometric activation of **1b-ZrBn$_2$** is active for the oligomerization of 1-hexene. While chain termination (or transfer) occurs frequently, the resulting zirconium species remain active for

(48) Herzog, T. A.; Zubris, D. L.; Bercaw, J. E. *J. Am. Chem. Soc.* **1996**, *118*, 11988–11989.
(49) Lin, S.; Waymouth, R. M. *Macromolecules* **1999**, *32*, 8283–8290.
(50) Cheng, H. N.; Smith, D. A. *Macromolecules* **1986**, *19*, 2065–2072.

Table 2. Polymerization Runs with Zirconium Precatalysts (all runs were with 34 to 39 mL of liquid propylene (measured at 0 °C) in 3.0 + 0.7 mL of toluene)

run	precatalyst	precatalyst (mmol)	time (h)	MAO (g)	MAO (equiv)	polymer (mg)	activity (g/mol·h)
1	**1a-ZrBn$_2$**	0.007	0.5	0.207	500	202	5.8×10^4
2	**1a-ZrBn$_2$**	0.007	2	0.207	500	702	5.0×10^4
3	**1a-ZrBn$_2$**	0.007	2	0.207	500	322	2.3×10^4
4	**1a-ZrBn$_2$**	0.007	1.5	0.414	1000	11120	1.1×10^6
5	**1a-ZrBn$_2$**	0.0035	0.5	0.207	1000	71	4.1×10^4
6	**1a-ZrBn$_2$**	0.0035	0.5	0.414	2000	904	5.2×10^5
7	**1a-ZrBn$_2$**	0.0035	0.5	0.621	3000	1717	9.8×10^5
8	**1a-ZrBn$_2$**	0.0035	0.5	0.828	4000	404	2.3×10^5
9	**1b-ZrBn$_2$**	0.007	2	0.207	500	9573	6.8×10^5
10	**1b-ZrBn$_2$**	0.007	2	0.207	500	7096	5.1×10^5
11	**1b-ZrBn$_2$**	0.0035	0.5	0.207	1000	2260	1.3×10^6
12	**1b-ZrBn$_2$**	0.0035	0.5	0.207	1000	1940	1.1×10^6
13	**1b-ZrBn$_2$**	0.0035	0.5	0.207	1000	2610	1.5×10^6
14	**2-ZrBn$_2$**	0.0007	0.5	0.207	5000	417	1.2×10^6
15	**2-ZrBn$_2$**	0.0007	0.5	0.207	5000	1621	4.6×10^6
16	**3-ZrBn$_2$**	0.007	0.5	0.414	1000	3260	9.3×10^5
17	**3-ZrBn$_2$**	0.007	0.5	0.207	500	5620	1.6×10^6

oligomerization for extended periods of time and even after the monomer is essentially consumed.

Complexes **2-ZrBn$_2$** and **3-ZrBn$_2$** show high polymerization activity as well upon activation with MAO. Complex **3-ZrBn$_2$** leads to stereoirregular polymers with a small amount of olefin and *n*-propyl end groups (^{13}C NMR spectrum, see Supporting Information). GC analysis shows the absence of low MW propylene oligomers. Contrastingly, polymerization trials with **2-ZrBn$_2$** lead to abundant formation of oily oligomers along with some higher polymers. A roughly statistical distribution of C_9 to C_{45} oligomers was observed by GC and GC-MS analysis in this case. ^{13}C NMR spectra of these samples show peaks attributable to olefin carbons and *n*-propyl terminal groups.

These results, while not well understood, show that changing the nature of the linker leads to differences in the outcome of propylene polymerizations. This feature provides opportunities for further studies of the role of different ligand characteristics on the produced polymer.

Propylene Polymerization and Oligomerization with Titanium Complexes. Propylene polymerization of the bis(phenolate)donor titanium dibenzyl complexes, upon activation with excess MAO, has been investigated (Table 3). Titanium bis(phenolate)pyridine systems were found to be about 3 orders of magnitude less active than the zirconium counterparts. One

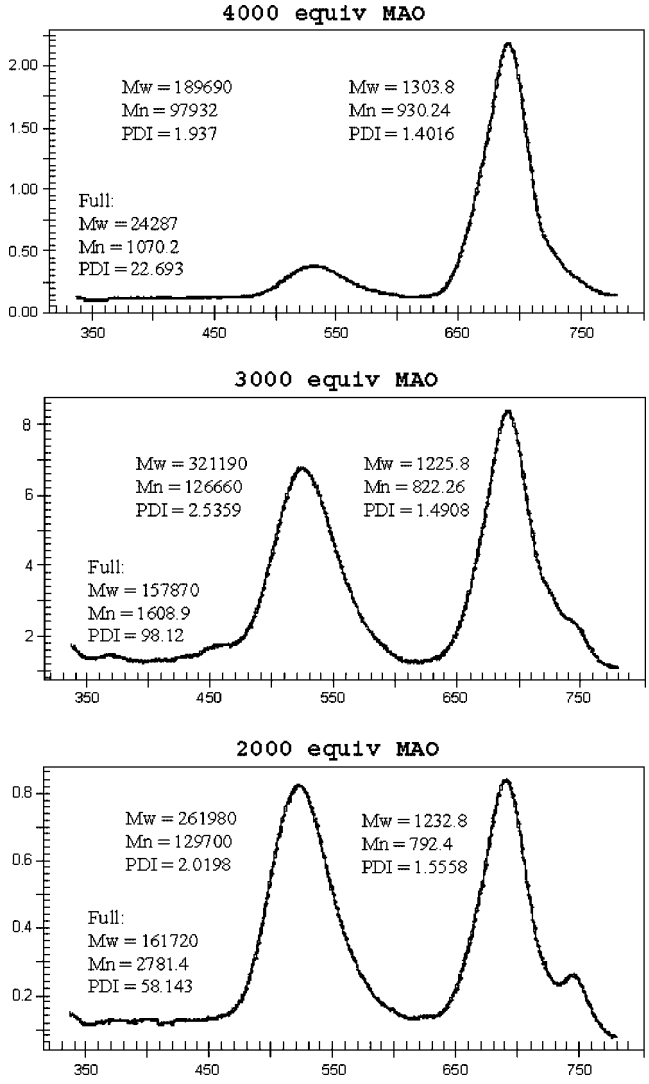

Figure 6. GPC for polymers obtained from **1a-ZrBn$_2$** upon activation with MAO (runs 6−8, Table 2).

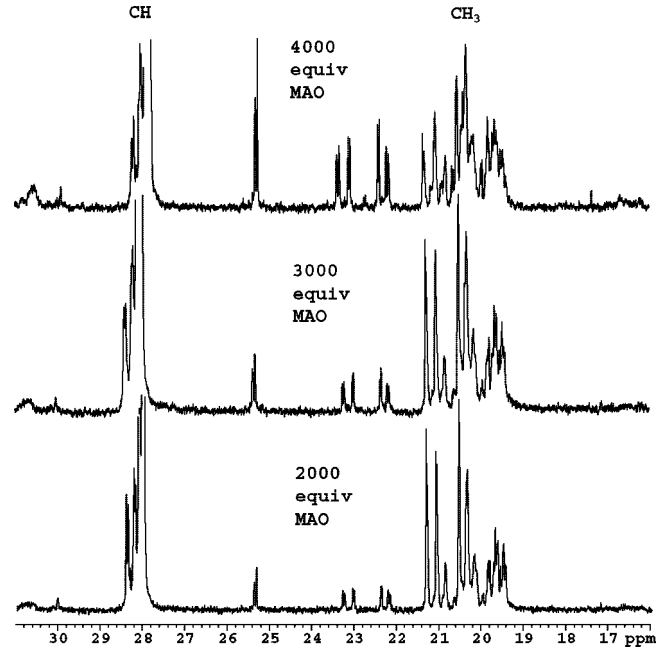

Figure 7. Selected region of ^{13}C NMR spectra for polymers obtained from **1a-ZrBn$_2$** upon activation with MAO (runs 6−8, Table 2). The peaks between 22 and 24 ppm correspond to isobutyl *C*H$_3$ groups, and the peaks between 24 and 25 ppm correspond to isobutyl *C*H groups.

Scheme 4

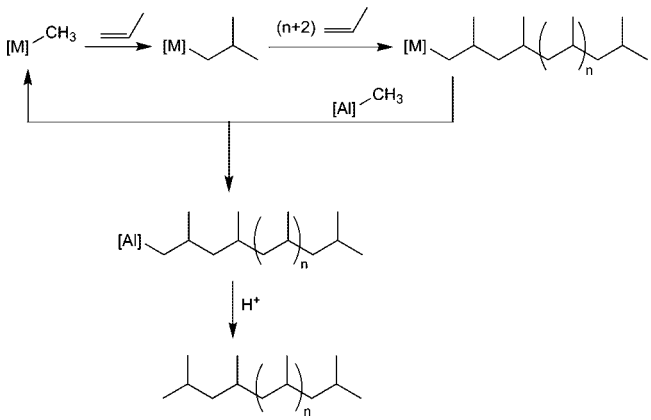

polymer sample, obtained in quantities sufficient for analysis, indicated that the polymer has a high molecular weight and shows no detectable olefin signals in the ^{13}C NMR spectra. The methyl region of the ^{13}C NMR spectrum shows a significant peak corresponding to the [*mmmm*] pentad overlapping with a distribution of peaks corresponding to essentially stereoirregular polypropylene.[51] Varying the solvent from toluene to chlorobenzene did not influence activity significantly. The observed lower activity compared to zirconium could be attributed to a more crowded environment around the titanium center. While the dibenzyl species may not be perfect models for the active catalysts, analysis of their solid-state structures may still hint at the features that control reactivity in these systems, in particular with regard to the ancillary ligand framework. Comparing the solid-state structures of **1b-ZrBn$_2$** and **1b-TiBn$_2$** shows that the zirconium center accommodates a sixth ligand in its coordination sphere, unlike titanium. A more open metal center could possibly allow for more facile propylene insertion and also for β-H elimination, which are observed for zirconium. Furthermore the zirconium precursor is C_s-symmetric while the titanium one is C_2-symmetric. The symmetry of the titanium system may have contributed to the observed fraction containing isotactic enrichment. It is important to note that while the precursors are well defined, the active cationic species are not and may have coordination numbers and geometries different from the ones observed in the precursors.

Titanium complexes supported by the furan (**2-TiBn$_2$**) and thiophene (**3-TiBn$_2$**) linked frameworks show high activity for the oligomerization of propylene. The oligomer products separate as oils upon quenching the MAO with HCl/MeOH and have been analyzed by GC, GC-MS, and NMR spectroscopy. The furan system was found to generate mainly C_9 to C_{21} oligomers, while the thiophene one generates a broader distribution of oligomers: C_9 to C_{33}. ^{13}C NMR spectra of the resulting oligomer mixtures show many olefin peaks along with a complicated aliphatic region. The complex spectra may be due to titanium chain-walking or to isomerization by acid catalysis during workup. Clearly, β-H elimination is a facile process in these systems. The increased activity of **2-TiBn$_2$** and **3-TiBn$_2$** compared to the pyridine-based systems may be due to a more open metal center. This is apparent in the solid-state structures of **2-TiBn$_2$** and **1a-TiBn$_2$**. Compared to the pyridine system (**1a-TiBn$_2$**), the furan-based system (**2-TiBn$_2$**) shows a significant increase in the distance between the bulky *ortho-tert*-butyl groups from 9.1 to 11.3 Å. This "opening" of the metal center could lead to faster insertion rates as well as the increased propensity for β-H elimination, both phenomena being observed.

Conclusions

Zirconium and titanium complexes supported by new tridentate, LX_2-type bis(phenolate)donor ligands have been prepared and investigated for applications in propylene polymerization. The ligand architecture has been varied by changing the donor linker from pyridine, to furan, to thiophene and the size of the subtituents *ortho* to the phenol oxygen. The zirconium and titanium dibenzyl species have been prepared by toluene elimination. The solid-state structures for the titanium complexes are roughly C_2-symmetric, while the zirconium ones are C_s- and C_1-symmetric. Both titanium and zirconium complexes were found to be active for the polymerization of propylene upon activation with MAO. The activities observed for the zirconium complexes are excellent, exceeding 10^6 g polypropylene/(mol Zr·h) in some cases. The excess of MAO was found to affect the polymerization activity and the level of β-H elimination and chain transfer events. Titanium bis(phenolate)pyridine systems are about 10^3 less active, but generate polymers of higher molecular weight. The titanium bis(phenolate)furan and bis(phenolate)thiophene systems were found to be active for propylene oligomerization catalysis. While in some cases the observed catalytic behavior could be explained by catalyst structure and reaction conditions, there are still features not well understood. Further exploration of related systems should lead to a better understanding of the important characteristics of these catalysts for controlling the polymer properties.

Experimental Section

General Considerations and Instrumentation. All air- and moisture-sensitive compounds were manipulated using standard vacuum line, Schlenk, or cannula techniques or in a drybox under a nitrogen atmosphere. Solvents for air- and moisture-sensitive reactions were dried over sodium benzophenone ketyl or by the method of Grubbs.[52] Benzene-d_6 was purchased from Cambridge Isotopes and distilled from sodium benzophenone ketyl. Chloroform-d_1 and chlorobenzene-d_5 were purchased from Cambridge Isotopes and distilled from calcium hydride. Phenols **1a-H$_2$**, **1b-H$_2$**, **2-H$_2$**, and **3-H$_2$** and their precursors have been prepared using procedures developed before.[53] Other materials were used as received. ^1H and ^{13}C NMR spectra were recorded on Varian Mercury 300 or Varian INOVA-500 spectrometers and unless otherwise indicated at room temperature. Chemical shifts are reported with respect to internal solvent: 7.16 and 128.38 (t) ppm (C_6D_6); 7.27 and 77.23 (t) ppm ($CDCl_3$); 5.32 and 54.00 (q) ppm (CD_2Cl_2); 6.0 and 73.78 (t) ppm ($C_2D_2Cl_4$); for ^1H and ^{13}C data.

Preparation of Ar′(OSEM). A procedure similar to the preparation of **Ar′(OMOM)** was utilized.[53] Yield: 90% (16.9 g) starting from 2-bromo-4,6-di-*tert*-butylphenol. ^1H NMR (300 MHz, $CDCl_3$) δ: 0.07 (s, 9H, Si(CH_3)$_3$), 1.06 (s, 2H, OCH$_2$CH_2Si), 1.30 (s, 9H, C(CH_3)$_3$), 1.44 (s, 9H, C(CH_3)$_3$), 3.98 (s, 2H, OCH_2CH$_2$Si), 5.26 (s, 2H, OCH_2O), 7.31 (d, 2H, aryl-*H*), 7.40 (d, 2H, aryl-*H*). ^{13}C NMR (75 MHz, $CDCl_3$) δ: −1.2 (Si(CH_3)$_3$), 18.4 (SiCH_2), 31.1 (C(CH_3)$_3$), 31.5 (C(CH_3)$_3$), 34.8 (C(CH$_3$)$_3$), 36.1 (C(CH$_3$)$_3$), 67.8 (OCH_2CH$_2$), 97.8 (OCH_2O), 117.8, 124.1, 128.9, 144.6, 147.6, 150.7 (aryl).

Preparation of Protected Diphenols. A Negishi coupling procedure was employed.[53]

(51) This polymer has been shown to be a mixture of highly isotactic and stereoirregular polypropylenes: Golisz, S. R.; Bercaw J. E. Manuscript in preparation.

(52) Pangborn, A. B.; Giardello, M. A.; Grubbs, R. H.; Rosen, R. K.; Timmers, F. J. *Organometallics* **1996**, *15*, 1518–20.

(53) Agapie, T.; Bercaw, J. E. *Organometallics* **2007**, *26*, 2957–2959.

Table 3. Polymerization Runs with Titanium Precatalysts (all runs were with 34 to 39 mL of liquid propylene (measured at 0 °C), 0.007 mmol of precatalyst, and 207 mg of MAO (500 equiv))[a]

run	precatalyst	time (h)	solvent (3 + 0.7 mL)	polymer (mg)	activity (g/mol·h)
1	**1a-TiBn$_2$**	0.5	toluene	3	8.6×10^2
2	**1a-TiBn$_2$**	0.5	toluene	2	5.7×10^2
3	**1a-TiBn$_2$**	2.6	toluene	14	7.7×10^2
4	**1a-TiBn$_2$**	2	toluene	8	5.7×10^2
5	**1a-TiBn$_2$**	2	toluene	7	5.0×10^2
6	**1a-TiBn$_2$**	2	chlorobenzene	17	1.2×10^3
7	**1a-TiBn$_2$**	2	chlorobenzene	20	1.4×10^3
8	**1b-TiBn$_2$**	2	toluene	35	2.5×10^3
9	**1b-TiBn$_2$**	2	toluene	32	2.3×10^3
10	**1b-TiBn$_2$**	2	chlorobenzene	30	2.1×10^3
11	**1b-TiBn$_2$**	2	chlorobenzene	30	2.1×10^3
12	**2-TiBn$_2$**[a]	0.5	toluene	870	2.5×10^5
13	**2-TiBn$_2$**[a]	0.5	toluene	1570	4.5×10^5
14	**3-TiBn$_2$**[a]	2	toluene	1940	1.4×10^5
15	**3-TiBn$_2$**[a]	2	toluene	2130	1.5×10^5

[a] Oligomers are obtained for these runs.

Table 4. Crystal and Refinement Data for Complexes 1b-ZrBn$_2$, 3-ZrBn$_2$, 1a-TiBn$_2$, 1b-TiBn$_2$, and 2-TiBn$_2$

	1b-ZrBn$_2$	**3-ZrBn$_2$**	**1a-TiBn$_2$**	**1b-TiBn$_2$**	**2-TiBn$_2$**
empirical formula	$C_{51}H_{67}NO_3Zr \cdot C_4H_{10}O$	$C_{46}H_{56}O_2SZr \cdot 1.5(C_7H_8)$	$C_{47}H_{57}NO_2Ti$	$C_{47}H_{57}NO_2Ti$	$C_{46}H_{56}O_3Ti$
fw	907.40	902.39	715.8	715.84	704.81
T, K	100(2)	100(2)	100(2)	208(2)	100(2)
a, Å	15.8272(11)	32.9618(13)	11.2513(4)	9.6700(6)	9.5660(14)
b, Å	16.9637(11)	10.8886(4)	13.1612(4)	19.2570(12)	14.100(2)
c, Å	19.1982(12)	28.8405(12)	13.7639(4)	21.9500(14)	15.100(2)
α, deg			76.075(1)		85.053(3)
β, deg	107.911(3)	107.7780(10)	81.769(1)	102.2860(10)	76.411(3)
γ, deg			84.868(1)		85.591(3)
volume, Å^3	4904.7(6)	9856.8(7)	1954.7(1)	3993.8(4)	1969.0(5)
Z	4	8	2	4	2
cryst syst	monoclinic	monoclinic	triclinic	monoclinic	triclinic
space group	$P2_1/n$	$C2/c$	$P\bar{1}$ (# 2)	$P2(1)/c$	$P\bar{1}$ (# 2)
d_{calc}, g/cm^3	1.229	1.216	1.216	1.191	1.189
θ range, deg	1.64 to 28.40	1.65 to 33.99	1.83 to 39.06	2.12 to 28.24	1.94 to 33.27
μ, mm^{-1}	0.269	0.305	0.258	0.252	0.256
abs corr	none	none	none	semiempir from equiv	TWINABS
GOF	1.128	1.258	1.329	1.035	1.730
R_1,[a] wR_2[b] [$I > 2\sigma(I)$]	0.0468, 0.0731	0.0485, 0.0821	0.0471, 0.0966	0.0448, 0.1168	0.0516, 0.1067

[a] $R_1 = \sum||F_o| - |F_c||/\sum|F_o|$. [b] $wR_2 = [\sum[w(F_o^2 - F_c^2)^2]/\sum[w(F_o^2)^2]]^{1/2}$.

1a-(MOM)$_2$. ^{1}H NMR (300 MHz, $CDCl_3$) δ: 1.37 (s, 18H, C(CH_3)$_3$), 1.51 (s, 18H, C(CH_3)$_3$), 3.41 (s, 6H, OCH_3), 4.64 (s, 4H, OCH_2O), 7.45 (d, 2H, aryl-*H*), 7.61 (d, 2H, aryl-*H*), 7.68−7.80 (m, 3H, NC$_5H_3$). ^{13}C NMR (75 MHz, $CDCl_3$) δ: 31.1 (C(*C*H$_3$)$_3$), 31.6 (C(*C*H$_3$)$_3$), 34.8 (*C*(CH$_3$)$_3$), 35.6 (*C*(CH$_3$)$_3$), 57.6 (O*C*H$_3$), 99.7 (O*C*H$_2$O), 123.2, 125.2, 126.7, 134.1, 136.1, 142.5, 146.1, 151.5, 158.4 (aryl).

1b-Me$_2$. ^{1}H NMR (300 MHz, $CDCl_3$) δ: 0.70 (t, 9H, CH$_2$CH_3), 1.85 (q, 6H, CH_2CH$_3$), 2.37 (s, 3H, aryl-CH_3), 3.32 (s, 6H, OCH_3), 7.05 (d, 2H, aryl-*H*), 7.42 (d, 2H, aryl-*H*), 7.65−7.75 (m, 3H, NC$_5H_3$). ^{13}C NMR (75 MHz, $CDCl_3$) δ: 8.7 (CH$_2$*C*H$_3$), 21.4 (aryl-*C*H$_3$), 27.1 (*C*H$_2$CH$_3$), 44.9 (aryl-*C*), 61.0 (O*C*H$_3$), 123.0, 130.2, 131.0,132.4, 134.2, 136.2, 138.7,155.8,158.2 (aryl).

2-(SEM)$_2$. ^{1}H NMR (300 MHz, $CDCl_3$) δ: 0.02 (s, 9H, Si(CH_3)$_3$), 0.97 (s, 2H, OCH$_2$CH_2Si), 1.34 (s, 9H, C(CH_3)$_3$), 1.48 (s, 9H, C(CH_3)$_3$), 3.83 (s, 2H, OCH_2CH$_2$Si), 4.93 (s, 2H, OCH_2O), 6.95 (s, 2H, OC$_4H_2$), 7.34 (d, 2H, aryl-*H*), 7.65 (d, 2H, aryl-*H*). ^{13}C NMR (75 MHz, $CDCl_3$) δ: −1.2 (Si(*C*H$_3$)$_3$), 18.4 (Si*C*H$_2$), 31.2 (C(*C*H$_3$)$_3$), 31.6 (C(*C*H$_3$)$_3$), 34.8 (*C*(CH$_3$)$_3$), 35.7 (*C*(CH$_3$)$_3$), 67.7 (O*C*H$_2$CH$_2$), 97.0 (O*C*H$_2$O), 111.3, 123.4, 124.4, 124.8, 143.1, 146.0, 150.3, 150.7 (aryl).

3-(MOM)$_2$. ^{1}H NMR (300 MHz, $CDCl_3$) δ: 1.35 (s, 18H, C(CH_3)$_3$), 1.50 (s, 18H, C(CH_3)$_3$), 3.51 (s, 6H, OCH_3), 4.80 (s, 4H, OCH_2O), 7.28 (s, 2H, SC$_4H_2$), 7.31 (d, 2H, aryl-*H*), 7.38 (d, 2H, aryl-*H*). ^{13}C NMR (75 MHz, $CDCl_3$) δ: 31.1 (C(*C*H$_3$)$_3$), 31.7 (C(*C*H$_3$)$_3$), 34.8 (*C*(CH$_3$)$_3$), 35.7 (*C*(CH$_3$)$_3$), 57.7 (O*C*H$_3$), 98.5 (O*C*H$_2$O), 124.5, 126.5, 127.0, 128.2, 141,8, 143.0, 146.2, 151.1 (aryl).

Removal of MOM Protecting Group.[53] Preparation of 1a-H$_2$ and 3-H$_2$. 1a-H$_2$. ^{1}H NMR (300 MHz, $CDCl_3$) δ: 1.39 (s, 18H, C(CH_3)$_3$), 1.48 (s, 18H, C(CH_3)$_3$), 7.46 (d, 2H, aryl-*H*), 7.51 (d, 2H, aryl-*H*), 7.67 (d, 2H, 3,5-NC$_5$H-H_2), 8.01 (t, 1H, 4-NC$_5H_2$-*H*), 10.59 (s, 2H, O*H*). ^{13}C NMR (75 MHz, $CDCl_3$) δ: 29.8 (C(*C*H$_3$)$_3$), 31.8 (C(*C*H$_3$)$_3$), 34.6 (*C*(CH$_3$)$_3$), 35.6 (*C*(CH$_3$)$_3$), 120.5, 121.3, 123.0, 126.4, 137.5, 140.0, 141.5, 153.3, 157.6 (aryl). HRMS C$_{33}H_{45}O_2N$: calcd mass 487.3450, measured mass 487.3446. Yield: 74% over two steps.

3-H$_2$. ^{1}H NMR (300 MHz, C_6D_6) δ: 1.30 (s, 18H, C(CH_3)$_3$), 1.61 (s, 18H, C(CH_3)$_3$), 5.57 (s, 2H, O*H*). 6.72 (s, 2H, SC$_4H_2$), 7.41 (d, 2H, aryl-*H*), 7.54 (d, 2H, aryl-*H*). ^{13}C NMR (75 MHz, $CDCl_3$) δ: 29.9 (C(*C*H$_3$)$_3$), 31.8 (C(*C*H$_3$)$_3$), 34.6 (*C*(CH$_3$)$_3$), 35.4 (*C*(CH$_3$)$_3$), 120.4, 125.0, 125.4, 127.3, 136.0 (aryl). HRMS C$_{32}H_{44}O_2S$: calcd mass 492.3062, measured mass 492.3067. Yield: 69% over two steps.

Removal of Methyl Protecting Group.[53] Preparation of Biphenol 1b-H$_2$. ^{1}H NMR (300 MHz, $CDCl_3$) δ: 0.71 (t, 9H, CH$_2$CH_3), 1.90 (q, 6H, CH_2CH$_3$), 2.35 (s, 3H, aryl-CH_3), 7.10 (d, 2H, aryl-*H*), 7.28 (d, 2H, aryl-*H*), 7.63 (d, 2H, NC$_5$H-3,5-H_2), 7.96 (t, 1H, NC$_5H_2$-4-*H*), 10.55 (br s, 2H, O*H*). ^{13}C NMR (75 MHz, $CDCl_3$) δ: 8.8 (CH$_2$*C*H$_3$), 21.4 (aryl-*C*H$_3$), 26.2 (*C*H$_2$CH$_3$), 44.9 (aryl-*C*), 120.2, 121.6, 126.5, 127.7, 132.9, 134.4, 140.0, 153.4, 157.3 (aryl). HRMS C$_{33}H_{45}O_2N$: calcd mass: 487.3450, measured mass 487.3460. Yield: 54% over two steps.

Removal of SEM Protecting Group. Preparation of Biphenol 2-H$_2$. Compound **2-(SEM)$_2$** (1.5 g, 2 mmol, 1 equiv) was dissolved in HMPA (50 mL) and a THF solution of Bu$_4$NF (1 M in THF

with 5% water, 20.4 mL, 10 equiv). The color of the mixture gradually changed from colorless to orange to green. After 2 days of stirring at room temperature, water was added and an CH_2Cl_2 extraction was performed. Organic fractions were dried over $MgSO_4$ and filtered, and volatile materials were removed by rotary evaporation. Remaining HMPA was removed by Kugelrohr distillation. Recrystallization from CH_3CN provides **3C** as a white powder (0.7645 g, 1.6 mmol, 80% yield). ^{1}H NMR (500 MHz, $CDCl_3$) δ: 1.35 (s, 18H, C(CH_3)$_3$), 1.48 (s, 18H, C(CH_3)$_3$), 6.58 and 6.79 (s, 2H each, O*H* and OC_4H_2), 7.35 (d, 2H, aryl-*H*), 7.39 (d, 2H, aryl-*H*). ^{13}C NMR (125 MHz, $CDCl_3$) δ: 29.9 (C(CH_3)$_3$), 31.7 (C(CH_3)$_3$), 34.6 (C(CH_3)$_3$), 35.4 (C(CH_3)$_3$), 109.1, 116.6, 122.0, 125.0, 136.8, 142.7, 149.6, 152.1 (aryl). HRMS $C_{32}H_{44}O_3$: calcd mass 476.3290, measured mass 476.3314.

Preparation of Group 4 Dibenzyl Complexes. General Procedure. 1a-TiBn$_2$. An Et_2O (10 mL) solution of phenol **1a** (100 mg, 206 μmol, 1 equiv) was added to a solution of $TiBn_4$ (86 mg, 206 μmol, 1 equiv) in Et_2O (5 mL). The mixture was stirred at room temperature for 5−12 h. Volatile materials were removed under vacuum, and the residue was mixed with petroleum ether and recrystallized at −35 °C. The desired product was collected by filtration and washed with cold petroleum ether. This procedure gives 130 mg (181 μmol, 87%) of **1a-TiBn$_2$** as an orange powder. ^{1}H NMR (500 MHz, CD_2Cl_2) δ: 1.41 (s, 18H, C(CH_3)$_3$), 1.94 (s, 18H, C(CH_3)$_3$), 3.48 (s, 4H, TiCH_2), 6.29−6.37 (m, 6H, *m*- and *p*-C_6H_2-H_3), 6.43 (d, 4H, *o*-C_6H_3-H_2), 7.16 (d, 2H, aryl-*H*), 7.43 (d, 2H, 3,5-NC_5H-H_2), 7.65 (t, 1H, 4-NC_5H_2-*H*), 7.68 (d, 2H, aryl-*H*). No distereotopic hydrogens are observed at −80 °C. −CH_2 give a singlet. ^{13}C NMR (125 MHz, CD_2Cl_2) δ: 31.5 (C(CH_3)$_3$), 32.0 (C(CH_3)$_3$), 35.0 (C(CH_3)$_3$), 36.2 (C(CH_3)$_3$), 84.5 (TiCH_2), 122.8, 123.9, 126.1, 127.0, 127.2, 127.8, 129.4, 136.0, 138.3, 138.5, 141.7, 156.5, 157.3 (aryl). Anal. Calcd for $C_{47}H_{57}NO_2Ti$ (%): C, 78.86; H, 8.03; N, 1.96. Found: C, 77.62; H, 8.38; N, 1.95.

1b-TiBn$_2$. ^{1}H NMR (500 MHz, C_6D_6) δ: 1.03 (t, 18H, CH_2CH_3), 2.34 (s, 6H, aryl-CH_3), 2.58 (q, 12H, CH_2CH_3), 3.83 (s, 4H, TiCH_2), 6.32 (t, 2H, *p*-C_6H_3-H_2), 6.51 (t, 4H, *m*-C_6H_3-H_2), 6.71 (t, 1H, 4-NC_5H_2-*H*), 6.77 (d, 4H, *o*-C_6H_3-H_2), 6.91 (d, 2H, 3,5-NC_5H-H_2), 6.93 (d, 2H, aryl-*H*), 7.43 (d, 2H, aryl-*H*). ^{13}C NMR (125 MHz, C_6D_6) δ: 9.4 (CH_2CH_3), 21.8 (aryl-CH_3), 27.3 (CH_2CH_3), 44.9 (aryl-*C*), 84.6 (TiCH_2), 123.2, 124.0, 127.9, 128.1, 128.6, 130.0, 130.2, 133.4, 133.8, 137.6, 138.8, 157.2, 157.5 (aryl). Anal. Calcd for $C_{47}H_{57}NO_2Ti$ (%): C, 78.86; H, 8.03; N, 1.96. Found: C, 78.53; H, 8.25; N, 2.10. Yield: 78%.

2-TiBn$_2$. ^{1}H NMR (500 MHz, C_6D_6) δ: 1.37 (s, 18H, C(CH_3)$_3$), 2.12 (s, 18H, C(CH_3)$_3$), 3.89 (s, 4H, TiCH_2), 6.37 (t, 2H, *p*-C_6H_3-H_2), 6.51−6.54 (m, 6H, overlap *m*-C_6H_3-H_2 and OC_4-H_2), 6.99 (d, 4H, *o*-C_6H_3-H_2), 7.49 (d, 2H, aryl-*H*), 7.73 (d, 2H, aryl-*H*). ^{13}C NMR (125 MHz, C_6D_6) δ: 32.0 (C(CH_3)$_3$), 32.1 (C(CH_3)$_3$), 35.0 (C(CH_3)$_3$), 36.6 (C(CH_3)$_3$), 88.2 (TaCH_2), 108.7, 121.3, 122.1, 124.1, 124.5, 128.4, 130.6, 137.9, 138.0, 143.1, 154.2, 155.7 (aryl). ^{13}C NMR (125 MHz, $CDCl_3$) δ: 31.5 (C(CH_3)$_3$), 31.9 (C(CH_3)$_3$), 34.8 (C(CH_3)$_3$), 36.1 (C(CH_3)$_3$), 87.4 (TiCH_2), 108.2, 120.7, 121.3, 123.3, 123.9, 127.9, 129.6, 137.2, 137.7, 142.7, 153.5, 155.0 (aryl). Yield: 62%.

3-TiBn$_2$. ^{1}H NMR (500 MHz, C_6D_6) δ: 1.33 (s, 18H, C(CH_3)$_3$), 2.06 (s, 18H, C(CH_3)$_3$), 3.93 (s, 4H, TiCH_2), 6.23 (s, 2H, SC_4H_2), 6.56 (t, 2H, *p*-C_6H_3-H_2), 6.3−6.5 (v br s, 4H, *m*-C_6H_3-H_2 or *o*-C_6H_3-H_2), 6.6−7.2 (v br s, 4H, *m*-C_6H_3-H_2 or *o*-C_6H_3-H_2), 7.41 (d, 2H, aryl-*H*), 7.74 (d, 2H, aryl-*H*). ^{1}H NMR (500 MHz, CD_2Cl_2) δ: 1.38 (s, 18H, C(CH_3)$_3$), 1.95 (s, 18H, C(CH_3)$_3$), 3.58 (br s, 4H, TiCH_2), 6.30 (s, 2H, SC_4H_2), 6.4−7.0 (br, 10H, C_6H_5), 7.27 (d, 2H, aryl-*H*), 7.56 (d, 2H, aryl-*H*). ^{13}C NMR (125 MHz, CD_2Cl_2) δ: 31.9 (C(CH_3)$_3$), 32.0 (C(CH_3)$_3$), 34.9 (C(CH_3)$_3$), 36.6 (C(CH_3)$_3$), 88.4 (TiCH_2), 122.9, 124.0, 125.7, 126.3, 127.2, 128.7, 131.2, 135.5, 137.7, 139.9, 142.9, 160.5 (aryl). This was obtained as a glassy material, which precluded recrystallization.

1a-ZrBn$_2$. ^{1}H NMR (500 MHz, C_6D_6) δ: 1.39 (s, 18H, C(CH_3)$_3$), 1.79 (s, 18H, C(CH_3)$_3$), 2.70 (s, 4H, ZrCH_2), 6.63 (t, 2H, *p*-C_6H_3-H_2), 6.78 (t, 4H, *m*-C_6H_3-H_2), 6.83 (t, 1H, 4-NC_5H_2-*H*), 7.02 (d, 4H, *o*-C_6H_3-H_2), 7.06 (d, 2H, 3,5-NC_5H-H_2), 7.10 (d, 2H, aryl-*H*), 7.70 (d, 2H, aryl-*H*). ^{13}C NMR (125 MHz, C_6D_6) δ: 31.1 (C(CH_3)$_3$), 32.3 (C(CH_3)$_3$), 34.9 (C(CH_3)$_3$), 36.0 (C(CH_3)$_3$), 60.1 (ZrCH_2), 123.3, 124.8, 126.4, 127.5, 129.7, 130.1, 136.3, 139.0, 139.1, 141.7, 155.1, 160.5 (aryl). Yield: 88%.

1b-ZrBn$_2$. ^{1}H NMR (500 MHz, C_6D_6) δ: δ: 0.92 (t, 18H, CH_2CH_3), 2.29 (s, 6H, aryl-CH_3), 2.33 (q, 12H, CH_2CH_3), 2.83 (s, 4H, ZrCH_2), 6.53 (t, 2H, *p*-C_6H_3-H_2), 6.72 (t, 4H, *m*-C_6H_3-H_2), 6.79 (d, 2H, aryl-*H*), 6.83 (app t, 1H, 4-NC_5H_2-*H*), 6.94 (d, 2H, 3,5-NC_5H-H_2), 6.97 (d, 4H, *o*-C_6H_3-H_2), 7.29 (d, 2H, aryl-*H*). ^{13}C NMR (125 MHz, C_6D_6) δ: 9.3 (CH_2CH_3), 15.7, 21.6 (aryl-CH_3), 26.9 (CH_2CH_3), 45.4 (aryl-*C*), 61.2, 66.1, 123.1, 125.3, 127.9, 129.0, 129.7, 129.9, 131.0, 133.3, 133.5, 138.8, 138.9, 155.1, 160.0 (aryl). Yield: 58%.

2-ZrBn$_2$. ^{1}H NMR (500 MHz, C_6D_6) δ: 1.38 (s, 18H, C(CH_3)$_3$), 1.76 (s, 18H, C(CH_3)$_3$), 2.51 (s, 4H, ZrCH_2), 6.53 (s, 2H, OC_4H_2), 6.67 (t, 2H, *p*-C_6H_3-H_2), 6.82 (t, 4H, *m*-C_6H_3-H_2), 7.03 (d, 4H, *o*-C_6H_3-H_2), 7.48 (d, 2H, aryl-*H*), 7.59 (d, 2H, aryl-*H*). ^{13}C NMR (125 MHz, C_6D_6) δ: 31.0 (C(CH_3)$_3$), 32.1 (C(CH_3)$_3$), 34.9 (C(CH_3)$_3$), 36.1 (C(CH_3)$_3$), 61.4 (ZrCH_2), 109.7, 121.4, 122.3, 124.1, 124.7, 129.6, 130.4, 137.5, 142.6, 152.9, 156.2 (aryl). Yield: 69%.

3-ZrBn$_2$. ^{1}H NMR (500 MHz, CD_2Cl_2) δ: 1.35 (s, 18H, C(CH_3)$_3$), 1.63 (s, 18H, C(CH_3)$_3$), 2.28 (br s, 4H, ZrCH_2), 6.51 (s, 2H, SC_4H_2), 6.68 (br s, 4H, *o*-C_6H_3-H_2), 6.85 (br t, 4H, *m*-C_6H_3-H_2), 6.99 (t, 1H, *p*-C_6H_4-*H*), 7.29 (d, 2H, aryl-*H*), 7.42 (d, xH, aryl-*H*). ^{13}C NMR (125 MHz, CD_2Cl_2) δ: 31.0 (C(CH_3)$_3$), 31.8 (C(CH_3)$_3$), 34.8 (C(CH_3)$_3$), 36.2 (C(CH_3)$_3$), 62.7 (ZrCH_2), 123.2, 123.9, 124.6, 125.5, 128.0, 130.0, 130.3, 137.5, 138.5, 142.4, 158.0 (aryl). Yield: 58%.

Preparation of (1a)$_2$-Ti. An Et_2O (3 mL) solution of $TiBn_4$ (12.7 mg, 30.8 μmol, 1 equiv) was added to a solution of **1a** (30 mg, 61.6, μmol, 2 equiv) in Et_2O (3 mL). The reaction mixture was allowed to stir at room temperature for 5 h. Then volatile materials were removed under vacuum and the residue was analyzed by ^{1}H NMR spectroscopy to show the presence of **1a-TiBn$_2$** and **1a-H$_2$**. The crude residue was dissolved in toluene and transferred to a Schlenk tube equipped with a screw-on Teflon stopper. The reaction flask was immersed in an oil bath at 60 °C and allowed to stir for 10.5 h. ^{1}H NMR spectrum of the residue upon volatile removal showed one major species, but the reaction still was not complete. The reaction mixture was resubmitted to heating with stirring for 24 h. Volatile materials were removed *in vacuo*. The residue shows clean formation of a species consistent with the formulation **(1a)$_2$-Ti** by ^{1}H and ^{13}C NMR spectroscopy. ^{1}H NMR (500 MHz, C_6D_6) δ: 1.02 (s, 18H, C(CH_3)$_3$), 1.42 (s, 18H, C(CH_3)$_3$), 7.28 (t, 1H, NC_5H_2-*H*), 7.55 (d, 2H, aryl-*H*), 7.64 (d, 2H, NC_5H-H_2), 7.76 (d, 2H, aryl-*H*). ^{13}C NMR (125 MHz, C_6D_6) δ: 29.9 (C(CH_3)$_3$), 32.3 (C(CH_3)$_3$), 34.9 (C(CH_3)$_3$), 35.3 (C(CH_3)$_3$), 123.2, 125.4, 126.1, 126.6, 135.8, 139.0, 140.7, 155.9, 160.2 (aryl).

Preparation of (1a)$_2$-Zr. An Et_2O (3 mL) solution of $TiBn_4$ (14 mg, 30.8 μmol, 1 equiv) was added to a solution of **1a** (30 mg, 61.6, μmol, 2 equiv) in Et_2O (3 mL). The reaction mixture was allowed to stir at room temperature for 5 h. Then volatile materials were removed under vacuum and the residue was analyzed by ^{1}H NMR spectroscopy. Compounds **1a-ZrBn$_2$**, **1a-H$_2$**, and **(1a)$_2$-Zr** can be identified by ^{1}H NMR spectroscopy. The crude residue was dissolved in toluene and transferred to a Schlenk tube equipped with a screw-on Teflon stopper. The reaction flask was immersed in an oil bath at 60 °C and allowed to stir for 10.5 h. ^{1}H NMR spectrum of the residue upon volatile removal shows clean formation of a species consistent with the formulation **(1a)$_2$-Zr** by ^{1}H and ^{13}C NMR spectroscopy. ^{1}H NMR (500 MHz, C_6D_6) δ: 1.17 (s, 18H, C(CH_3)$_3$), 1.43 (s, 18H, C(CH_3)$_3$), 7.21 (t, 1H, NC_5H_2-*H*), 7.47 (d,, 2H, NC_5H-H_2), 7.59 (d, 2H, aryl-*H*), 7.67 (d, 2H, aryl-

H). ^{13}C NMR (125 MHz, C_6D_6) δ: 30.2 ($C(CH_3)_3$), 32.3 ($C(CH_3)_3$), 34.9 ($C(CH_3)_3$), 35.6 ($C(CH_3)_3$), 123.7, 125.6, 125.7, 127.2, 138.1, 139.6, 140.4, 156.8, 157.3 (aryl).

General Polymerization Procedure. A high-pressure glass reactor was charged with solid MAO (0.207 to 0.828 mg, 500 to 4000 equiv), and toluene (3 mL, distilled from Na/Ph_2CO) was added. The vessel was sealed and attached to a propylene tank and purged. Upon cooling to 0 °C, propylene (35−39 mL) was condensed in. Zirconium or titanium precatalysts (0.7−7 μmol) were added via syringe, as a toluene solution (0.7 mL). The reaction mixture was stirred vigorously at 0 °C for the desired amount of time. Excess propylene was carefully vented. Then the cold bath was removed, and a MeOH/HCl solution (10:1, 50 mL) was added slowly. The resulting mixture was transferred to an Erlenmeyer flask, additional MeOH/HCl solution was added (50 mL), and the mixture was allowed to stir at room temperature for at least 4 h. The methanol solution was decanted and the polymer was rinsed with methanol. Upon decanting the methanol, the polymer was trasfered to a vial, and volatile materials were removed by placing the vial under vacuum and heating to 80 °C. The resulting materials were investigated by NMR spectroscopy and GPC. Polymer NMR spectroscopy data were acquired at 115 °C. If oligomers rather than polymers were formed, the MeOH/HCl solution was extracted with pentane twice. *tert*-Butylbenzene (0.5 mL) was added to the combined organics, and the mixture was investigated by GC and GC-MS. No polymer was formed without titanium or zirconium precatalyst addition.

X-ray Crystal Data: General Procedure. Crystals grown from diethyl ether (**1b-ZrBn$_2$**), toluene (**3-ZrBn$_2$**), or a mixture of diethyl ether and petroleum ether (**1a-TiBn$_2$**, **1b-TiBn$_2$**, and **2-TiBn$_2$**) at −35 °C were removed quickly from a scintillation vial to a microscope slide coated with Paratone N oil. Samples were selected and mounted on a glass fiber with Paratone N oil. Data collection was carried out on a Bruker Smart 1000 CCD diffractometer. The structures were solved by direct methods. All non-hydrogen atoms were refined anisotropically. Some details regarding refined data and cell parameters are available in Table 4. Selected bond distances and angles are supplied in the captions of Figures 1−5.

Acknowledgment. This work has been supported by the USDOE Office of Basic Energy Sciences (Grant No. DE-FG03-85ER13431). The authors thank Michael Day (Caltech) for assistance in obtaining the X-ray crystal structures. We are grateful to Mona Shahgholi (Caltech) for help with HRMS and Sara Klamo (Dow) for obtaining the GPC data.

Supporting Information Available: Tables of bond lengths, angles, and anisotropic displacement parameters for the presented solid-state structures. VT ^{1}H NMR spectra of **1a-TiBn$_2$**. ^{1}H and ^{13}C NMR spectra for all reported compounds. Representative ^{13}C NMR spectra of polymer samples (PDF). X-ray crystallographic data (CIF). This material is available free of charge via the Internet at http://pubs.acs.org.

OM800136Y